

Expanded View Figures

Figure EV1. QUIPPER assay, example plate maps.

- A Western Blot analysis of chronically RML6-infected CAD5 cells following PK digestion. Anti-PrP antibody POM1 is used for probing the membrane. Brain homogenates were used as controls.
- B Western Blot analysis of chronically RML6-infected GT-1/7 cells after PK treatment. Membrane is probed with anti-PrP antibody POM1. Brain homogenates were used as controls.
- C Western blot analysis of infected and uninfected CAD5 and GT-1/7 cells following PIPLC treatment and subsequent PK digestion. Membranes are probed with anti-PrP antibody POM1. α : anti-actin antibody is used to probe the membrane as loading control.
- D Plate map used in the screen depicting controls and samples. Light green represents wells containing siRNAs from the library, dark green represents wells containing Prnp-targeting control siRNAs and yellow represents wells containing non-targeting control siRNAs.
- E Examples of heat maps for FRET as well as viability read-out from the primary screen.
- F Schematic of the hit-selection process over all the screens performed in this study with the corresponding criteria.

Source data are available online for this figure.

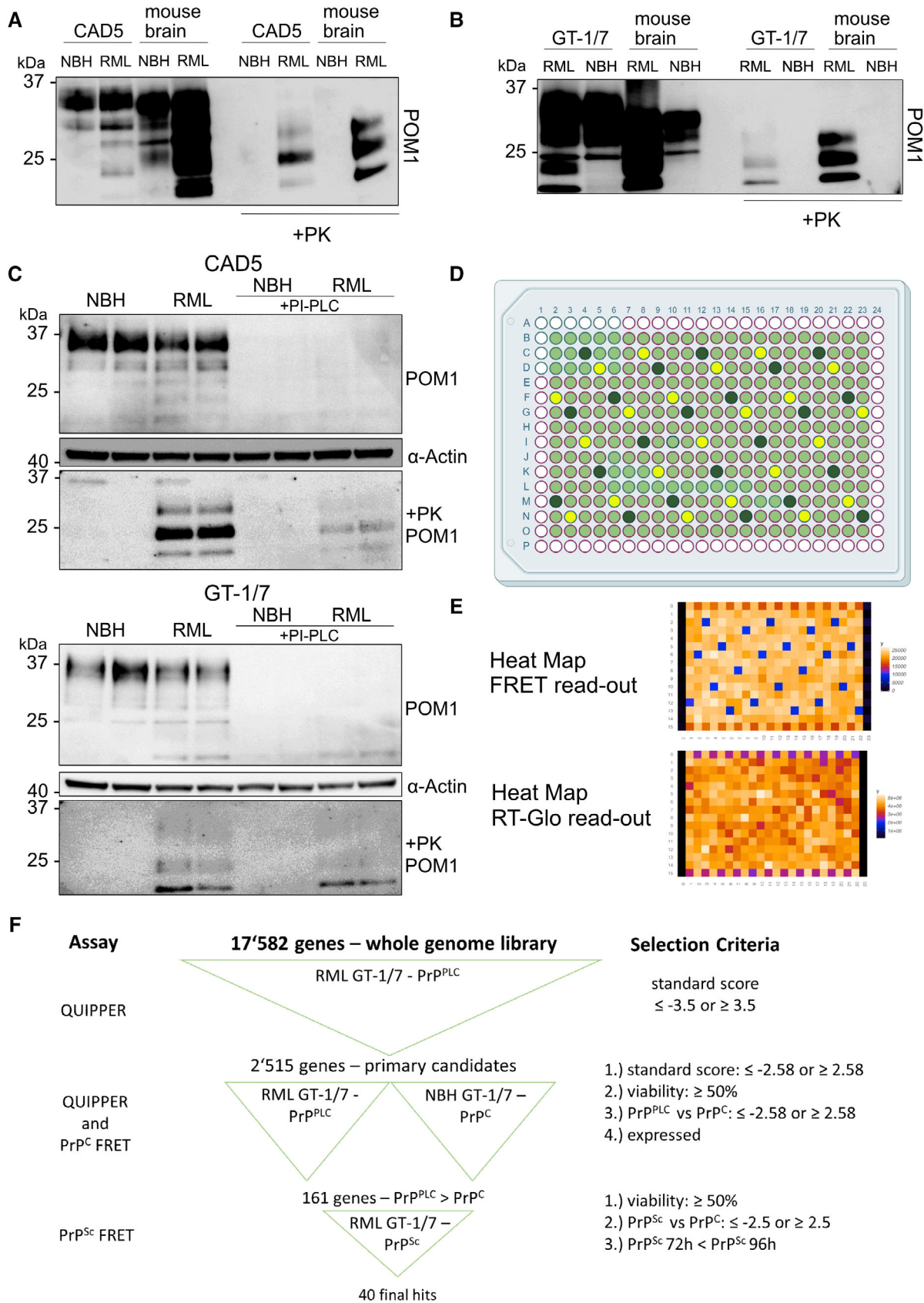


Figure EV1.

Figure EV2. Secondary screen quality metrics and viability readout.

- A Z'-factor for each plate of both deconvolution screens (for regulators of PrP^{PLC}, top panel, for regulators of PrP^C, bottom panel) representing the robustness of the screens based on the separability of the positive (*Prnp* targeting) and negative (non-targeting) control. 0.5–1 (green) = excellent assay, 0–0.5 (yellow) = acceptable assay, 0 \geq (red) = unacceptable assay.
- B Duplicate correlation of FRET-data for each screen. Coefficient of determination (r^2 -value) is depicted in the graph.
- C Duplicate correlation of viability-data measured using RealTime-Glo™ luminescence readout for each screen. Coefficient of determination (r^2 -value) is depicted in the graph.
- D Duplicates from (C) were averaged and normalized for each screen, and the two normalized values for each gene is correlated to assess if any gene regulates viability dependent on prion infection. The high r^2 -value, as well as the lack of outliers demonstrates the lack of synthetic lethal genes in the subset assessed in the deconvolution screen.

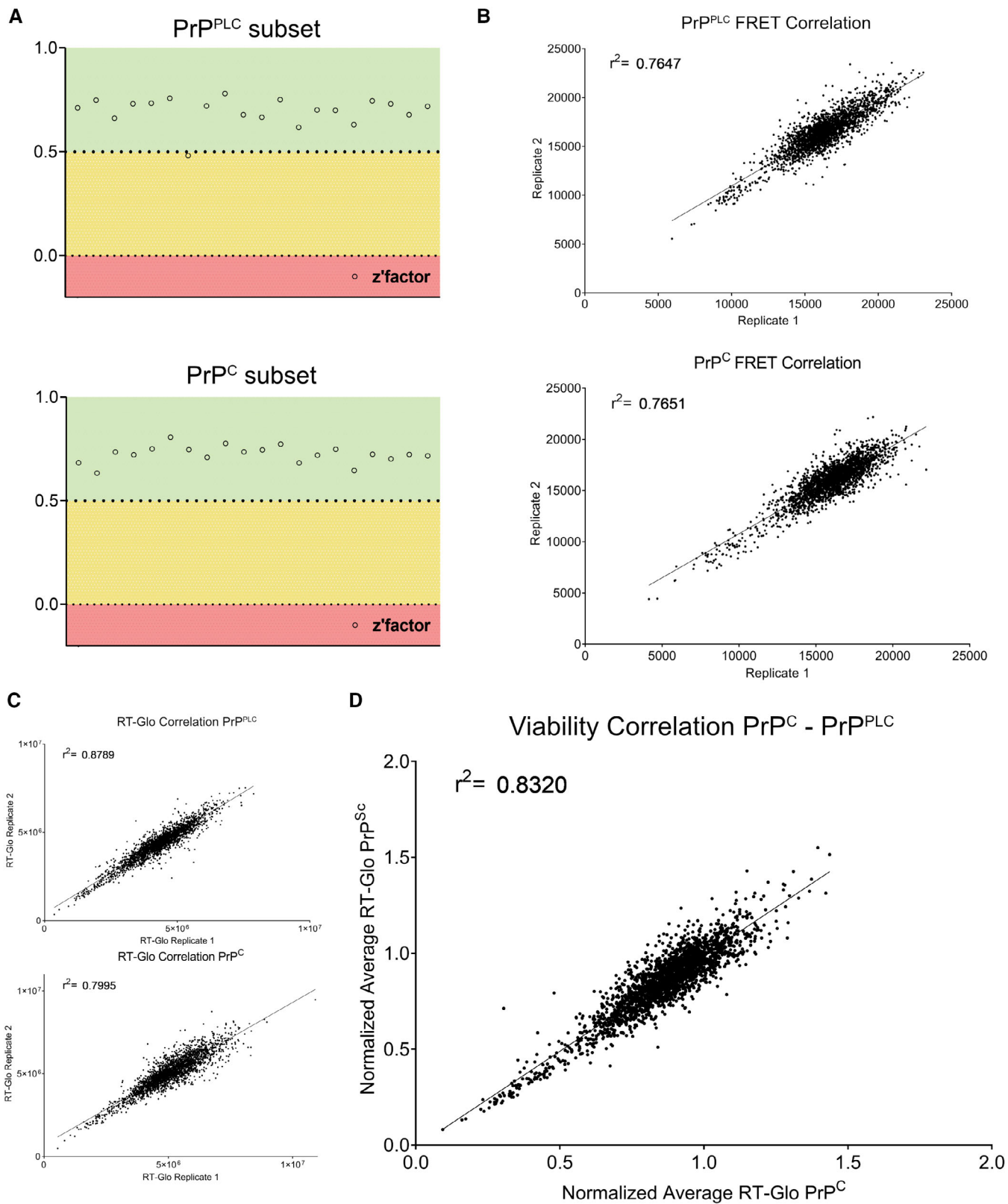


Figure EV2.

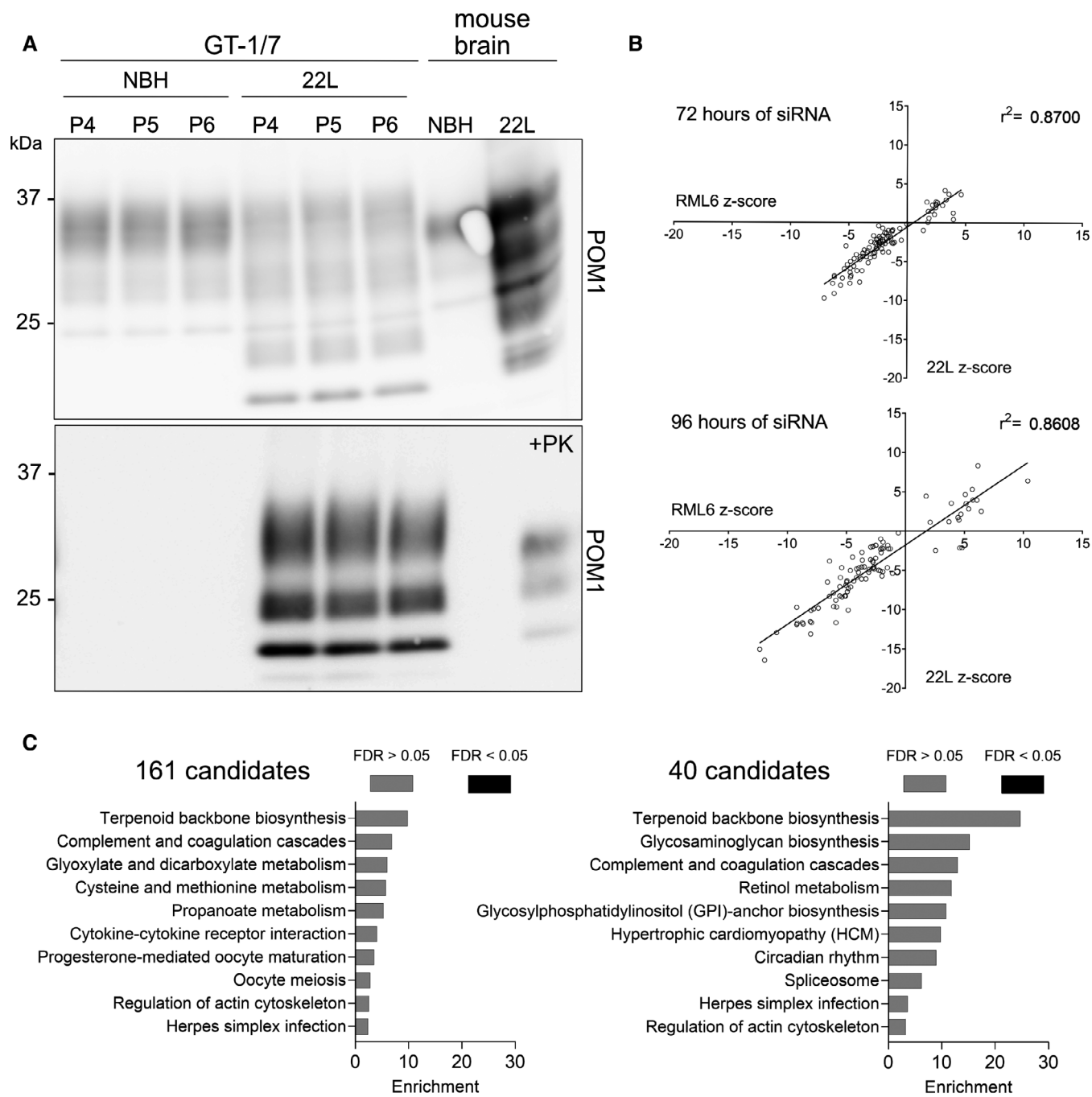


Figure EV3. Prion strain dependence of the 97 candidates.

A Western Blot analysis of chronically 22L-infected GT-1/7 cells after PK treatment. Membrane is probed with anti-PrP antibody POM1. P4, P5 and P6 corresponds to the amount of passaging after exposure to 22L brain homogenate. Brain homogenates were used as controls.

B Correlation of the effect of 97 candidates on their effect on PrP^{Sc} of two different prion strains (RML6 and 22L). Next to RML6 infected GT-1/7, 97 hits were assessed for their effect on 22L prion infected GT-1/7 for 72 h as well as 96 h-long treatment duration. The high coefficient of determination (r^2 -value) of the effect observed for both prion strains indicates that the candidates do not show strain-specificity.

C Gene set overrepresentation analysis for 161 hits and 40 hits from the prion modifier screen. No pathway passed the threshold for significance.

Source data are available online for this figure.

Figure EV4. Phenotypic response of PG127prion infected hovS upon HNRNPK downregulation using siRNA or shRNA.

- A Western blot showing *HNRNPK* siRNA transfection (96 h) decreases HNRNPK protein levels while it increases PrP^{Sc} in prion infected hovS cells. *PRNP* siRNAs suppressed both PrP^C and PrP^{Sc} as expected. α : anti Quantifications are reported as normalized to Actin and in comparison, to NT. PK-western blot is quantified relative to NT.
- B Brightfield microscopy images of the effect of siRNA mediated *HNRNPK* downregulation on vacuolation in PG127 and NBH hovS cells. Downregulation of *ovPRNP* in the infected hovS eliminates the vacuoles; *HNRNPK* downregulation in uninfected cells does not yield a vacuolation phenotype. Scale bar = 100 μ m.
- C Western Blot of PSA-treated uninfected and PG127 infected hovS cells. Increasing concentration of PSA leads to a more prominent reduction of PrP^{Sc}. PK-western blot is quantified relative to DMSO.
- D Western blot showing *HNRNPK* shRNA transduction (96 h) decreases HNRNPK protein levels while it increases PrP^{Sc} in PG127 prion infected hovS cells. α : anti. Quantifications are reported as normalized to Actin and in comparison, to NT. PK-western blot is quantified relative to NT.
- E Brightfield microscopy images of the effect of shRNA mediated *HNRNPK* downregulation on vacuolation in NBH hovS cells. *HNRNPK* downregulation in uninfected cells does not yield a vacuolation phenotype. Scale bar = 100 μ m.
- F Representative Western Blot analysis of the effect of 2 days of PSA treatment on PrP^{Sc} and HNRNPK levels in PG127 prion infected hovS cells following 96 h after transduction of control (NT) or *HNRNPK* targeting shRNAs. PSA treatment does not affect the levels of HNRNPK (upper panel) when compared with DMSO-treated cells. HNRNPK downregulation significantly increases PrP^{Sc} levels. α : anti. PK-western blot is quantified relative to DMSO NT samples. Data points represent individual experiments. ** $P = 0.0051$ (unpaired *t*-test).
- G Representative Western Blot analysis of the effect of 5 days of PSA treatment on PrP^{Sc} and HNRNPK levels in PG127 prion infected hovS cells following 168 h after transduction of control (NT) or *HNRNPK* targeting shRNAs. α : anti. PK-western blot is quantified relative to DMSO NT samples.
- H Heat map of the log₂ fold-change of functional targets of Hnrnpk upon siRNA or PSA treatment.

Source data are available online for this figure.

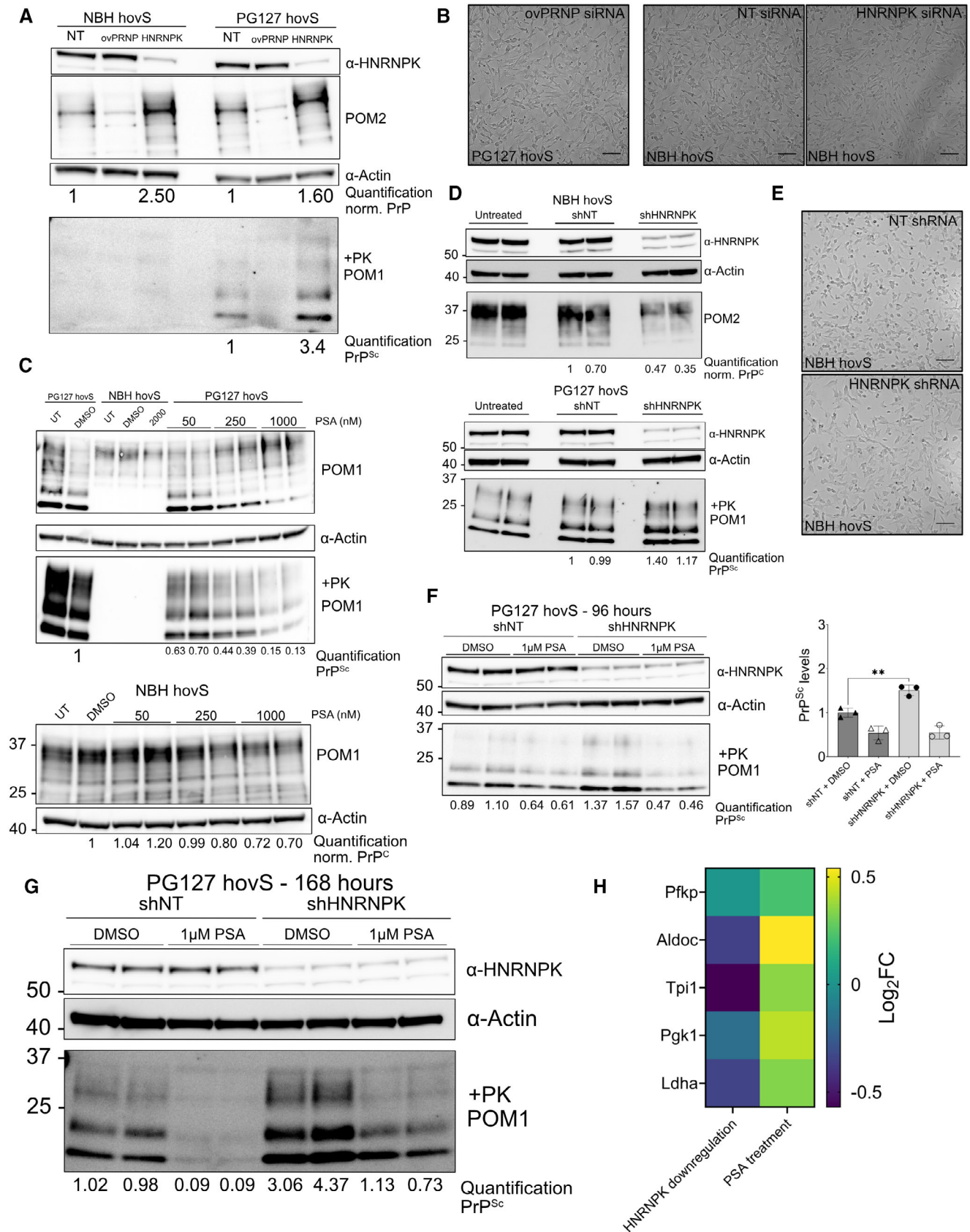


Figure EV4.